IEEE Access
Multidisciplinary | Rapid Review | Open Access Journal

Received June 21, 2018, accepted August 1, 2018, date of publication August 16, 2018, date of current version September 21, 2018.

Digital Object Identifier 10.1109/ACCESS.2018.2865808

General Synthesis Methodology for the Design of Acoustic Wave Ladder Filters and Duplexers

ALFRED GIMÉNEZ, JORDI VERDÚ, (Member, IEEE), AND PEDRO DE PACO SÁNCHEZ
Telecommunications and Systems Engineering Department, Universitat Autònoma de Barcelona, 08193 Barcelona, Spain

Corresponding author: Alfred Giménez (Alfred.Gimenez@uab.cat)

This work was supported by the Spanish Ministerio de Economía y Competitividad under Grant TEC2015-69229-R.

ABSTRACT In a scenario where the segment of wireless communication systems are allocated in an ever more crowded frequency spectrum, the design of filtering structures, stand-alone, duplexers, or multiplexers, become a challenging task. Moreover, filters based on acoustic wave resonators are the more suitable technology in this context due to the small size and the exhibited outstanding performance. However, to accommodate the technological requirements to the mask fulfillment is not straightforward unless a systematic synthesis methodology is used. Taking advantage on the nodal approach, the general synthesis methodology for ladder-type filters based on acoustic wave resonators is presented in this paper. This is a very fast procedure, which allow a better understanding of the interaction between technological constraints and filter performance. An experimental validation is proposed for a B28Rx band filter.

INDEX TERMS Bulk acoustic wave filters, duplexer, elliptic filters synthesis, extracted pole, non-resonating node (NRN), surface acoustic wave filters.

I. INTRODUCTION

Mobile communication is the key element to enable platforms for social innovative services and user applications, from both technological and an economical point of view. The general demand for mobile broadband data services is continuously growing, where mobile traffic has experimented a twofold growth each year, and will continue rising in the future fueled by ubiquity needs [1]. In this context, at the system level, duplexers but also multiplexers are key elements, where the number of services and roaming bands around the world is growing continuously [2]–[5]. On the other hand, the minimization of the occupied area of the filter is also a very important task in the filter design while improving the filter performance at the same time. This still more emphasized with the last developments of advanced LTE-Carrier Aggregation [6]–[8].

Indeed, filters and duplexers based on unbeatable advantages of micro-acoustic technologies, either based on surface or bulk acoustic waves, are on the rise because of the global transition to 5G networks [1], [2]. With the aim to meet the filter requirements such high selectivity, high rejection at adjacent bands or low insertion loss, more sophisticated filter techniques have to be developed [9]. However, it is also very important to consider the technological constraints which turns the design into a very complex and challenging task [10], [11]. The previous considerations lead to focus the problem from a methodological point of view. To do this, two different objectives have to be achieved: first, the definition of a network to fulfill the filter requirements, which has to be at the same time related with an equivalent circuit model for the parameter extraction. Second, the arrangement of the resonators in the network taking into consideration the technological constraints given by a specific material system definition.

Up to date, bandpass filter responses with transmission zeros at finite frequencies are well-known [12], [13]. The way to face the design of such networks can be understood from the lowpass model based on cross-couplings suggested in [14]–[16] or by the extracted pole technique. In both cases there are some inherent limitations which may be overcame by the use of non-resonating nodes as proposed in [17]–[20]. The proposed ladder-type network based on AW resonators can be understood as an in-line topology composed of extracted pole sections, where a resonant node is connected to a non-resonant node as it will be further discussed. This way to understand the network present some advantages: modularity, since each extracted pole section, that is each AW resonator, contributes with a finite transmission zero independently; and the possibility of having a fully canonical filter response without the traditional direct source to load coupling. In this case, this coupling is achieved by the reactive path through NRNs.

The goal of this work is to demonstrate that a general synthesis methodology can be used to design a ladder-type filter able to accommodate technological requirements based either in bulk acoustic wave (BAW) or surface acoustic wave (SAW) resonators [6], [21], [22]. In-line prototypes using non-resonating nodes are well studied, and the analytical solution can be found, which takes to the closed-equations for the definition of the elements of the lowpass prototype network. Therefore, from the lowpass prototype defined network, the extraction of the elements and the frequency transformation can be carried out to obtain the value of the required acoustic resonators to conform the bandpass RF filter.

The work has been organized as follows: the nodal representation in the low frequency domain of a ladder-type filter is presented in section III. The nature and meanings of the nodes are introduced in section III.A and the bandpass transformation is introduced in section III.B. The synthesis and parameter extraction of either stand-alone or duplexer lowpass prototype is carried out along section IV. In section V, an example of a B25 duplexer is carried out using the proposed synthesis methodology based on direct synthesis and equivalent models made up of resonating and non-resonating nodes. The example is used to show how the features of resonators, technology constraints, and the nature and values of external reactive elements can be taken into account and controlled with the methodology. As an experimental validation for the proposed synthesis methodology, a filter for the B28Rx band has been designed, simulated and compared with measurement demonstrated in section VI. Finally, the conclusions are presented.

II. STATE OF THE ART

The exhibited high performance of filters based on AW resonators is key for the development of wireless communications systems. Ladder topologies are quite popular with acoustic technologies, and they can implement a full filtering structure or can be combined with other topologies as well [23], [24]. The most common way to design a ladder-type filter based on AW resonators is based on the organization of consecutive series and parallel resonators considered as extracted-pole sections, defining a final network which will be solved through the use of numerical methods [25]–[27]. The main limitation is given by the need of bounding the electromechanical coupling coefficient, k^2_{eff}, or equivalently by the r capacitance factor, that is the static capacitance over the motional ratio [28], for each of the acoustic wave resonators in a specific margin. This can be controlled by the presence of external reactive elements. However, these can be also used to improve the filter response as proposed in [29].

In the case that the input/output phases are not properly considered, that is, the filtering function is not properly synthesized, an input/output reactive matching elements will be required. These external reactive elements can be avoided considering the proper input/output reflection phase condition [30].

A similar difficulty arises when two stand-alone filters are combined to set a duplexer, particularly when the duplexer channels are very close [2], [6], [31]. To avoid loading effects the use of matching networks have been widely explored [32], [33]. Since an AW filter can be designed to fulfill an open circuit boundary at Rx frequency band, the matching network at the Tx input path is usually unnecessary. However, at the antenna port, two different matching configurations can be used: in the Rx path the use of a $\lambda/4$ transmission line to obtain low impedance input at the Tx band; or the use of a PI-network formed by a series inductor between two parallel capacitors, replacing the previous $\lambda/4$ transmission line. The use of reactive elements allows further miniaturization, the shunt capacitors can be absorbed by the first input resonator and a series inductor remains in series over the Rx path [2].

However, the mutual loading effects, that are produced in the three-port junction, can be corrected by defining the proper input/output phase condition for each of the filters of the system. In this case, the out-of-band rejection can be improved, but also the minimum insertion loss. To do this, a shunt inductor is normally required at the antenna port to implement this phase correction [6], [7]. Depending on the frequency distance between bands and the allocation of the first transmission zero for each filter, the nature of this element may be capacitive. The proposed synthesis methodology is able to predict the reactive nature of such element.

III. LOWPASS AW LADDER-TYPE PROTOTYPE BASED ON THE NODAL REPRESENTATION

Characteristic generalized Chebyshev filtering functions can be accommodated by AW ladder-type networks. Moreover, fully canonical responses can be obtained with N finite transmission zeros, being N the order of the filter. This is achieved using the presence of the NRNs [17] without the requirement of the classical direct source to load coupling. As it was previously discussed, the extracted pole technique can be used to the synthesis of in-line structures with N transmission zeros. The lowpass prototype representation for acoustic wave filters is shown in Fig. 1, in which N sections of resonant nodes connected to a NRN through an admittance inverter are found.

A. LOWPASS EQUIVALENT BUTTERWORTH-VAN DYKE RESONATOR

It is widely accepted that the Butterworth-Van Dyke (BVD) electrical model, made of a series LC resonator in the motional arm in parallel with the static capacitance, is a faithful representation of the electrical behavior for piezoelectric resonators in the main resonance vicinity [21], [34]. The equivalent circuit includes technological constraints such as the electromechanical coupling constant k^2_{eff}. However, a lowpass prototype [10], [11] is required in order to use the characteristic polynomials which describes the generalized Chebyshev filtering function. The lowpass model is presented in Fig.2 for both the series and shunt resonator.

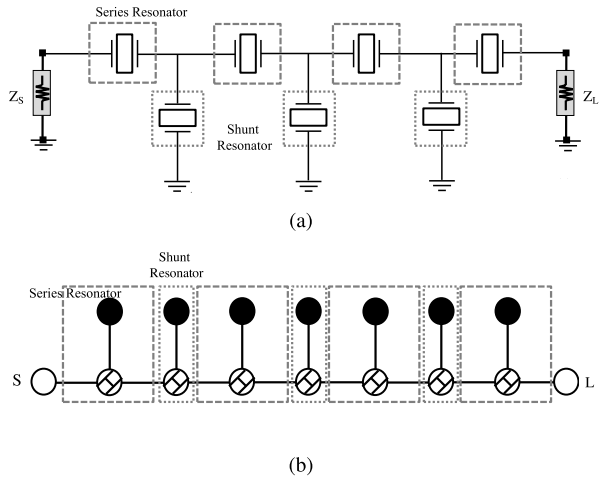

FIGURE 1. (a) Ladder-type network based on AW resonators. (b) Nodal representation of the circuit in (a) based on non-resonant (NRN) nodes.

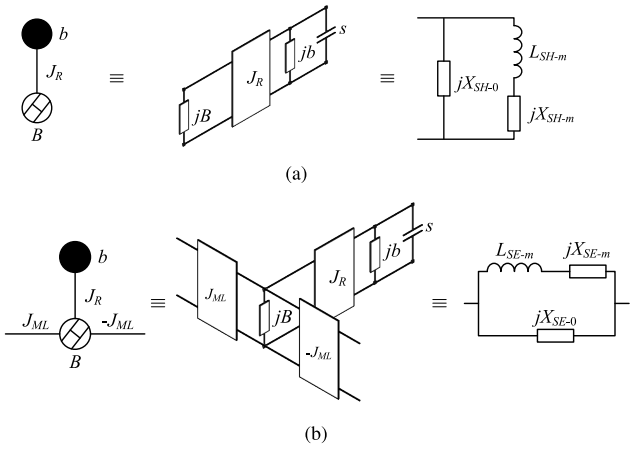

FIGURE 2. (left) Nodal representation, (center) Equivalent circuit schematic, and (right) Equivalent lowpass BVD model for: (a) Shunt resonator and (b) Series resonator.

The most basic resonant structure, which is a dangling resonator, is composed of a unitary capacitor, with admittance $Y = s$, in parallel with a constant susceptance b. Both are at the same time connected through an admittance inverter J_R to an NRN, which is implemented by means of a frequency invariant reactance (FIR) B. Each dangling resonator contributes with a specific attenuation pole. Therefore, for a fully canonical structure supporting n_{TZ} finite transmission zeros, $N = n_{TZ}$ dangling resonators must be found. The input admittance of the basic cell for the shunt resonator in Fig.2(a) is found to be:

$$y_i = jB_i + \frac{J_r^2}{s + jb_i} \tag{1}$$

Note that such admittance is infinite when $s = -jb_i$, that is at the position of the transmission zero at normalized frequency $\Omega_i = -b_i$. The sign of the transmission zero may be either positive or negative, resulting in a series or shunt resonator respectively after the network denormalization. On the other hand, for $y_i = 0$, an attenuation zero is produced, leading the signal to propagate from source to load through the NRN (B_i). Such admittance characteristics of dangling resonators are equivalent to those of a BVD model, but in lowpass normalized frequencies. This is further evidence of the equivalence of both circuits.

By proper inspection of this scenario, the closed-form expressions to relate the nodal elements with the elements corresponding to the lowpass BVD circuit can be established. In the case of the shunt resonator in Fig. 2(a) the FIR (B_i) can be directly related with X_{SH-0}. The remaining elements are found by the analysis of the acoustic branch formed by the series inductor and the FIR (X_{SH-m}). Therefore,

$$X_{SH-0} = -\frac{1}{B}; \quad X_{SH-m} = \frac{b}{J_R^2}; \quad L_{SH-m} = \Omega\frac{1}{J_R^2} \tag{2}$$

where Ω is the normalized frequency, and subscript m refer to motional (acoustic) branch. Since we are interested in the transformation of the network into a ladder structure, it is necessary to include admittance inverters on both sides of the resonator for the parameter extraction cell represented in Fig. 2(b). This is known as the serialization of the dangling resonator. The analysis of a dangling resonator placed between two admittance inverters results in the relation equations needed to transform it into a series lowpass equivalent circuit. In this case the elements are found to be:

$$X_{SE-0} = \frac{B}{J_{ML}^2}; \quad X_{SE-m} = \frac{B}{J_{ML}^2}\left(b\frac{B}{J_R^2} - 1\right)$$
$$L_{SE-m} = \Omega\frac{B}{J_{ML}^2}\frac{B}{J_R^2} \tag{3}$$

B. LOWPASS TO BANDPASS MODEL TRANSFORMATION

Once the lowpass prototype models have been obtained, frequency and impedance denormalization must be performed to obtain the bandpass BVD model. It is important to mention that at this point the proposed lowpass prototype satisfies the acoustic filter conditions in terms of frequency response. To obtain the elements of the bandpass filter, the bilateral lowpass-to-bandpass frequency transformation is applied [35]:

$$\Omega = \alpha\left(\frac{\omega}{\omega_0} - \frac{\omega_0}{\omega}\right); \quad \alpha = \frac{\omega_0}{\omega_2 - \omega_1} \tag{4}$$

where α is the inverse of the relative bandwidth, ω is the unnormalized frequency variable and ω_0 is the center frequency of the bandpass which has been calculated as the geometric mean of passband edges ω_1 and ω_2.

In order to relate the lowpass and bandpass circuit parameters shown in Fig. 3 the impedance and its derivative of both the lowpass and bandpass BVD model respectively must be equalized. The resulting relationships are:

$$L_A = \frac{1}{2}\left(\frac{2\alpha L_m + X_m}{\omega_0}\right)Z_0 \tag{5}$$

$$C_A = \frac{2}{\omega_0\left(2\alpha L_m - X_m\right)}\frac{1}{Z_0} \tag{6}$$

$$C_0 = -\frac{1}{\omega_0 X_0}\frac{1}{Z_0} \tag{7}$$

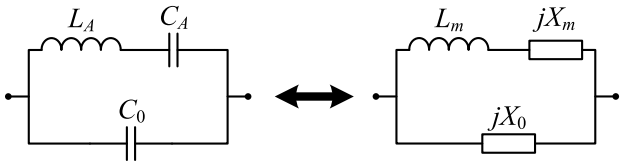

FIGURE 3. Lowpass and Bandpass BVD prototype of an acoustic wave resonator.

being Z_0 the reference impedance, L_A, C_A, and C_0 are the BVD model parameters; and L_m, X_m and X_0 are the lowpass prototype elements.

The electromechanical coupling coefficient settles the pole-zero distance of a resonator, and it depends basically on the material system and technology. Although this parameter is considered in the bandpass domain, the same definition can be applied to in the lowpass domain. Therefore, considering the relation between lowpass and bandpass parameters in (5-7), it is obtained for the series resonator:

$$rC_{SE} = \frac{C_A}{C_0} = 2\left.\frac{X_0/L_m}{X_0/L_m - 2\alpha}\right|_{SE} = -\left[\frac{B}{J_R^2}(2\alpha - b) + \frac{1}{2}\right] \tag{8}$$

and equivalently for the shunt resonator:

$$rC_{SH} = \frac{C_A}{C_0} = 2\left.\frac{X_0/L_m}{X_0/L_m - 2\alpha}\right|_{SH} = \frac{B}{J_R^2}(2\alpha - b) \tag{9}$$

By simple inspection it can be deduced that the relation between the r capacitance factor is inversely proportional to the electromechanical coupling coefficient, and also to the relative bandwidth. But this model embraces a more complex relation. Finally, to arrange a transmission zero above the filter passband, the reactance of the non-resonating node B should be negative (series resonator), and positive to place it below the passband (shunt resonator).

Although the transformation is very accurate around the central frequency ω_0, the fact of using FIR elements in the lowpass prototype entails by nature a certain limitation when they are transformed to the bandpass frequency domain at frequencies far away from ω_0, since now there is a frequency dependence not considered in the lowpass prototype. Direct bandpass synthesis may overcome this limitation, however, the method is restricted to a certain number of topologies [36].

IV. SYNTHESIS AND PARAMETER EXTRACTION

The generalized Chebyshev function is defined by a certain equiripple level in the bandpass, and a limited number of transmission zeros in the out-of-band region. The reflection and transmission response can be obtained as the ratio of two finite-degree polynomials, characteristic polynomials, and a real normalization constant [12], [37]. To perform the lowpass prototype element extraction the input admittance is required which is related to the reflection parameter $S_{11}(s)$, defined as a function of the characteristic polynomials as:

$$S_{11}(s) = e^{j\theta_{11}}\frac{F(s)}{\varepsilon_R E(s)} \tag{10}$$

where $F(s)$, $E(s)$, and ϵ_R, are obtained from the recursive method proposed by Cameron and Mansour in [12] which requires the allocation of the transmission zeros Ω_{ki}, the return loss level RL and the order of the filter N.

Since the phase term θ_{11} is a real quantity, the magnitude $|S_{11}|$ remains unaltered. However, this phase shift is required to avoid the use of external matching reactive elements when the first/last transmission zero is extracted [17], and the first element is a NRN, as it is the case of acoustic wave resonators [11].

In order to obtain the proper value of the phase term, we have to analyze the reflection parameter $S_{11}(s)$ at the position of the first transmission zero (normalized frequency $s = j\Omega_1$), where the input admittance results in $y_{in} = 0$. In this situation the signal will be reflected at the input port, that is $|S_{11}| = 1$. As suggested in [17], the phase term is calculated using:

$$e^{j\theta_{11}} = \left.\frac{\varepsilon_R E(s)}{F(s)}\right|_{s=j\Omega_1} \tag{11}$$

Once the reflection coefficient is fully determined, and considering the source and load terminations normalized to unity, the input admittance to the filter can be obtained as follows [38]:

$$y_{in} = \frac{1 - S_{11}(s)}{1 + S_{11}(s)} = \frac{\varepsilon_R E(s) - e^{j\theta_{11}}F(s)}{\varepsilon_R E(s) + e^{j\theta_{11}}F(s)} \tag{12}$$

A. PARAMETER EXTRACTION OF SYMMETRICAL STAND-ALONE FILTERS

Following the last procedure, the phase term should be properly introduced in order to avoid external input/output elements, due to the first element of the prototype is not a resonator, but a NRN connected to a dangling resonator. In Fig. 5 there is shown the inline nodal representation of an acoustic ladder filter of order N, without external input/output reactance due to its symmetry ($y_{in} = y_{out}$). In order to carry out the parameter extraction, the input admittance related with the characteristic polynomials in (12) must be equalized to the one of the network to be extracted. For the symmetrical network in Fig. 4 the input admittance is defined as:

$$y_{in}(s) = \cfrac{J_1^2}{jB_1 + \cfrac{J_{r1}^2}{s+jb_1} + \ldots + \cfrac{J_n^2}{jB_n + \cfrac{J_m^2}{s+jb_n} + \cfrac{J_{n+1}^2}{G_L}}} \tag{13}$$

The extraction process can be considered as a recursive method since the network is composed by a concatenation of extracted pole sections between admittance inverters. At the beginning of the process, for the first section shown in Fig.5(a), the input admittance is obtained as:

$$\frac{J_1^2}{y_{in}(s)} = \frac{J_{r1}^2}{s + jb_1} + jB_1 + y_1(s) \tag{14}$$

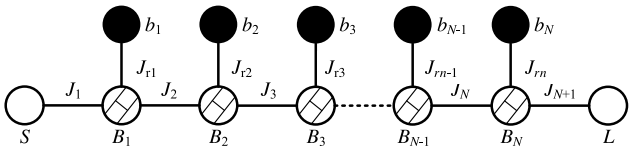

FIGURE 4. Nodal representation of the Lowpass prototype with degree *N*.

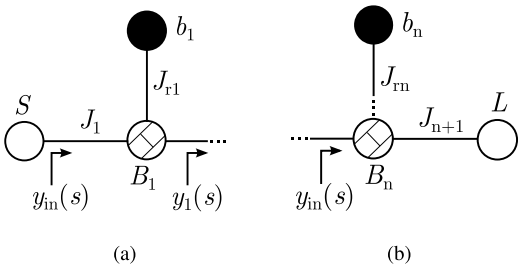

FIGURE 5. Equivalent nodal representation for the extraction: (a) of first fundamental element, and (b) last element in the circuit.

being $b_1 = -\Omega_1$ the normalized frequency of the transmission zero introduced by the first dangling resonator. Equation (14) can been rewritten as a partial fraction expansion, so the coupling J_{r1} can be easily extracted. This coupling is the residue of the admittance for the pole $-b_1$ and it can be obtained as:

$$J_{r1}^2 = (s - j\Omega_1)\frac{1}{y_{in}(s)}\bigg|_{s=j\Omega_1} \tag{15}$$

The reactance B_1 corresponding to the NRN is the last element to be extracted. This element will prepare the extraction of the next section. Therefore, it has to be obtained by evaluating the input admittance at the position of the following transmission zero, where $y_1(s) = 0$:

$$B = Im\left[y_{in}(s)|_{s=j\Omega_2}\right] \tag{16}$$

Once all the parameters of the fundamental elementary structure are extracted, the remaining admittance becomes the same as equation (14) for the following dangling resonator, and the extraction is also computed using equations (15) and (16). It has to be pointed out that the extraction can be carried out simultaneously from source to load and from load to source. For sake of clarity, in this work all the extractions are carried out from source to load. The remaining network once the last section has to be extracted is shown in Fig.5(b). In this case, the input admittance is calculated as:

$$y_{in}(s) = jB_n + \frac{J_{n+1}^2}{G_L} \tag{17}$$

In case of considering unitary load, that is $G_L = 1\Omega$, the real and imaginary part of the remaining admittance has to be absorbed by the last NRN B_n and the last coupling to load J_{n+1}^2. In the case of dealing with symmetrical networks, the last coupling is unitary. This is not the case for asymmetrical networks where external reactive elements might be used to have a unitary coupling. This is one of the conditions for dangling to acoustic resonator transformation.

This case is discussed later in this section. The general extraction technique used in this work was introduced taking into account general cases in [17].

B. PARAMETER EXTRACTION OF SYMMETRICAL DUPLEXERS

One of the main features in the duplexer design is the high isolation level between Tx and Rx bands. The incoming signal at the common port (antenna) for the Rx band is split up in the Rx and Tx paths. The signal propagating to the Tx is reflected back to the Rx path. With the aim to ensure signal integrity, such interference should be constructive. This situation is also given for a signal in the Tx band.

As it was previously discussed, the input phase for the filter is usually set to avoid the use of external matching reactive elements (11). However, this can be also designed to accomplish with a certain reflection condition at a certain frequency. In this case, the phase can be set for having $\angle S_{11} = 0°$ at the central frequency of the counter band f_{Dual} (Rx frequency at the Tx path, or Tx frequency at the Rx path). The phase adjustment at a frequency different of the position of the first transmission zero, as stated in (11), requires the presence of external matching reactive elements at the input/output ports [6], as is shown in Fig. 6. This is the reason of using external matching reactive elements in stand-alone filter for a not properly considered input phase.

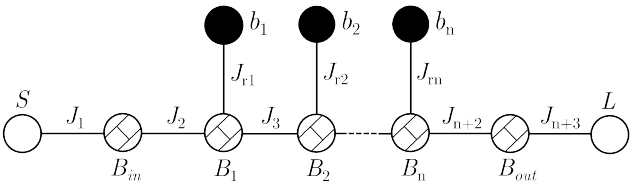

FIGURE 6. Lowpass prototype of one of the filters forming the duplexer, where input/output elements are needed for the phase correction.

The calculation of the input phase is similar to the case in equation (11), however in this case the evaluation is carried out at $s = j\Omega_{Dual}$. Regarding the extraction procedure, this is the same than the one for the case of stand-alone filter seen in section A, however now input and output reactance B_{in} and B_{out} must be taken into consideration for the extraction by using equation (16).

C. SYNTHESIS OF ASYMMETRICAL FILTERS AND DUPLEXERS

The methodology presented in this work considers the extraction of the different elements of the network from the source to the load. Therefore, the input admittance is calculated from the reflection parameter $S_{11}(s)$ with an appropriate phase term, but it does not consider the output reflection coefficient $S_{22}(s)$. In asymmetrical networks, where the input array of transmission zeros is not symmetrical, $\angle S_{11} \neq \angle S_{22}$, an external reactive element is required at the output to satisfy the

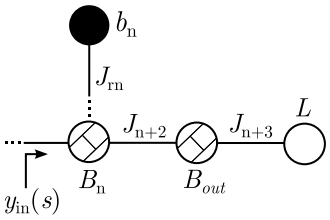

FIGURE 7. Last resonator and output FIR element to match the admittance and the phase of the reflection $S_{22}(s)$.

orthogonality condition between phases of $S_{11}(s)$, $S_{22}(s)$, and $S_{21}(s)$ [12], considering unitary source and load terminations.

In case the extraction is done simultaneously from source and load, one non-unitary coupling appears in the middle of the network. This situation is not considered since although in the framework of acoustic technologies it is straightforward to add an external output element, it can be intricate to introduce a coupling or lumped elements between resonators.

In case of asymmetrical duplexers, the external input/output reactance, and therefore the input/output external elements, are not equal. Thus, it is important to notice that $\angle S_{22} \neq 0°$ at f_{Dual}.

The extraction methodology for asymmetrical filters is the same as seen before, whether it is the design of a filter or a duplexer, until the extraction of the last non-resonant node B_n. The remaining network at that point is shown in Fig. 7 and the input admittance can be written as follows:

$$y_{in}(s) = jB_n + \frac{J_n^2}{jB_{out} + \frac{J_{n+1}^2}{G_L}} = jB_n + \frac{J_n^2}{jB_{out} + J_{n+1}^2 R_L} \tag{18}$$

Solving equation (18) for a pair of coupling values $J_n, J_{n+1} = 1$, the real and imaginary part of the input admittance can be obtained:

$$Re\,[y_{in}] = \frac{R_L}{B_{out}^2 + R_L^2}$$
$$Im\,[y_{in}] = B_n - \frac{B_{out}}{B_{out}^2 + R_L^2} \tag{19}$$

Considering that the load termination is unitary, the two NRNs are set by the real and imaginary parts of the remaining input admittance as:

$$B_{out} = \pm\sqrt{\frac{R_L - R_L^2 \cdot Re[y_{in}]}{Re[y_{in}]}}$$
$$B_n = Im[y_{in}] + \frac{B_{out}}{B_{out}^2 + R_L^2} \tag{20}$$

At this point, there is a trade off for the design of asymmetrical acoustic filters and duplexers. The advantage is that B_{out} can be chosen either positive or negative. Since B_n depends on it, the sign selection of B_{out} should be such that the resulting value of the coupling constant k_{eff}^2 is the most similar as the required one. In the case that $Re[y_{in}] > 1$, the resulting B_{out} is pure imaginary, likewise, a real FIR element if the load impedance is $R_L = 1$. This situation can be overcome by increasing the reactive element at the output of the filter, or designing the filter to be matched at the output to a termination impedance that results in real B_{out} in (20).

During the design of asymmetrical acoustic filters, some additional lumped element is usually required at the output port. Furthermore, we must be aware that it is possible that the load impedance cannot be 50 Ohms, but the one needed for the network synthesis to solve (20) obtaining B_{out} real.

V. CONSIDERATIONS OF THE TECHNOLOGICAL CONSTRAINTS IN THE DESIGN OF AW FILTERS AND DUPLEXERS

At this point the network elements have been extracted following the proposed synthesis methodology. The technological constraints inherent of the acoustic technology have not been yet considered, however, the methodology should be native oriented to accommodate the objective electromechanical coupling constant. A good practice about the effective coupling constant k_{eff}^2 that depends directly on the technology is to hold certain uniformity through the whole structure.

In the case of AW filters, the extracted pole sections contribute with a transmission zero at finite frequencies. That is, the classical General Chebyshev polynomials can be interpreted as a degenerated function where the transmission zeros allocated at infinite frequencies has been moved to finite positions, and the *RL* controls the in-band response. Therefore, the objective is focused in finding the return loss *RL* and the number and frequency allocation of the transmission zeros which results in a network which meets the specific technological constraints minimizing at the same time the number of external lumped elements.

There is not a unique way to obtain the most suitable set of finite transmission zeros and *RL* to accommodate the technological constraints. For a predefined array of transmission zeros, a sweep of *RL* show the better value to have the desired uniform electromechanical coupling constant for all the resonators (if possible). On the other hand, if the value of *RL* is predefined, a study of the allocation of Ω_i can be carried out to fulfill the maximum number of technological requirements with the minimum number of external elements.

To exemplify the kind of information that you can manage, it is worthy to observe results shown in Fig. 8. Here, the obtained values for k_{eff}^2 as a function of the specified *RL* are found. In this case $N = 7$ and $\Omega_1 = 1.62$, $\Omega_2 = -1.94$, $\Omega_3 = 1.71$, $\Omega_4 = -1.70$, $\Omega_5 = 1.71$, $\Omega_6 = -1.94$, and $\Omega_7 = 1.62$. The TZ are symmetrical, and a general case of $k_{eff}^2 = 7\%$ at 2 GHz has been considered for the study.

In this case, there is a specific value of $RL = 22$dB for which the value of k_{eff}^2 for each resonator is the same, that is, no external elements are needed to achieve the material system definition. If we try to synthesize this filter without this information, assigning an arbitrary return loss for those fixed transmission zeros, we would find that four lumped elements will be required; in particular, for resonators 1, 2, 6, and 7,

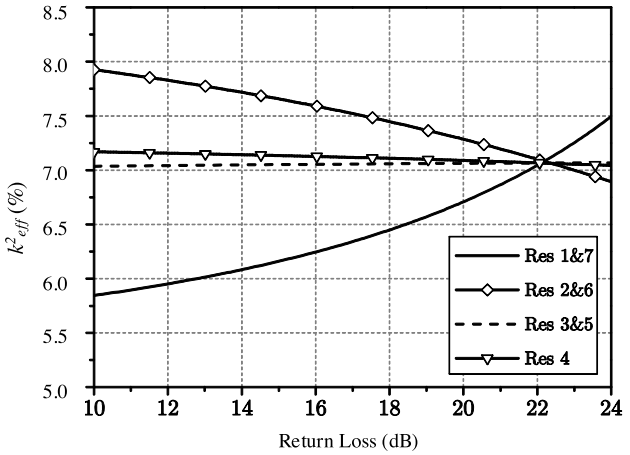

FIGURE 8. Obtained values of k^2_{eff} for each resonator as a function of *RL* for a predefined vector of transmission zeros.

since the value of k^2_{eff} for those resonators differs from the objective, which is not the case of resonators 3, 4 and 5 resulting in an almost constant $k^2_{eff} = 7\%$. Therefore, taking into consideration this information, a filter without any additional lumped element and satisfying the technological requirements can be achieved.

Similarly, the value of *RL* can be swept to obtain information about the resonant frequencies for each resonator, as it is shown in Fig. 9. However, this parameter is more dependent on filter specifications and technological requirements. The resonant frequency of series resonators is given by the synthesis and the resonant frequency of shunt resonators is directly related with the position of the transmission zero's frequency. Therefore, for a filter with the used predefined vector of transmission zeros, it is not possible to obtain uniform k^2_{eff} and only three different resonant frequencies at the same time.

Usually there is a trade off in most of the cases with respect the uniformity of k^2_{eff} and the number of required different resonant frequencies. In the same way, if resonators

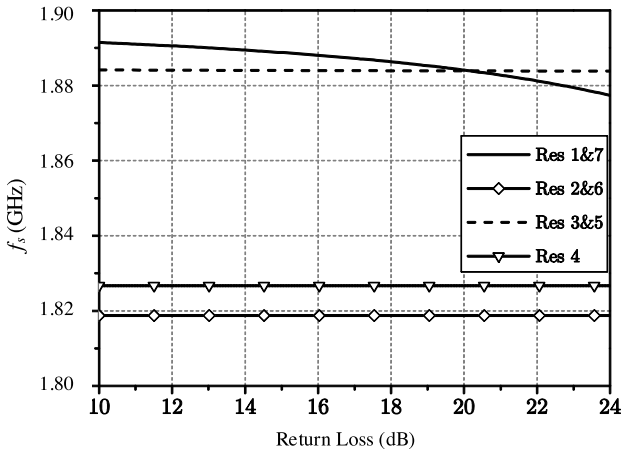

FIGURE 9. Obtained f_s as a function of *RL* for each resonator for a predefined vector of transmission zeros.

are deviated from the required k^2_{eff}, the allocation, nature, and value of the external reactive elements are completely controlled. This information has been used to underlay interesting experimental findings, reported for some authors, where they describe some advantages by enabling a subset of the resonators to work with a lower electromechanical coupling, thus improving the slope steepness of the filters [39].

A. EXAMPLE OF A DUPLEXER DESIGN

With the aim to validate the proposed methodology, a duplexer for the B25 Rx/Tx band is designed where the number of external reactive elements have been minimized while the mask fulfillment is achieved. The proposed methodology controls the nature and allocation of those external reactive elements to satisfy technological requirements. The specifications in terms of insertion loss, isolation and out-of-band rejection are shown in Table 1. The frequency distance between Tx and Rx bands is only of 15 MHz with a rejection of −50 dB. The design considers a state-of-art value of $k^2_{eff} = 6,7\%$.

TABLE 1. B25 Duplexer specifications.

Requirement	Freq. Band (MHz)	Value (dB)
Insertion Loss	1930 - 1995 (Rx)	<-2.5
	1850 - 1915 (Tx)	<-2
Isolation	1850 - 1915 (Rx)	>-50
	1930 - 1995 (Tx)	>-50
Out-of-band Rejection	1710 - 1755 (B4)	>-50

Before starting with the extraction process, the value for k^2_{eff} for a given vector of finite transmission zeros as a function of the *RL* value can be obtained to evaluate the need of external reactive elements. The spectrum mask is not considering neither temperature nor fabrication tolerances. Despite this simplification affects the example results, it does not affect the systematic methodology.

For the receiver filter the following configuration of normalized finite zeros is selected $[\Omega_1, \Omega_7] = 2.40$, $[\Omega_2, \Omega_6] = -1.89$, $[\Omega_3, \Omega_5] = 1.76$, and $\Omega_4 = -1.72$, for $RL = 18$ dB. In Fig. 10 there are represented the coupling constants for different *RL* values and the transmission zeros seen above. It can be seen that for $RL = 18$ dB no external elements are needed for any resonator of the Rx, since the coupling constant is uniform at $k^2_{eff} = 6.76\%$.

Since a duplexer is being designed, an input and output elements are required to impose zero-phase at Tx center frequency. Thus, the phase term of reflection parameter has to be evaluated at $f_{DualTx} = 1882$ MHz, which corresponds with the normalized frequency $\Omega_{DualTX} = -2.49$. This phase term in S_{11} is found to be $\theta_{11} = 44.07°$.

Using such phase term and the generated polynomials of generalized Chebyshev filtering function in (12), and following the extraction steps described in Section IV we get the following circuit elements: $B_1 = -1.4777$, $B_2 = 4.3881$, $B_3 = -1.5121$, $B_4 = 4.2762$, $J_{r1} = 1.6162$, $J_{r2} = 2.7261$,

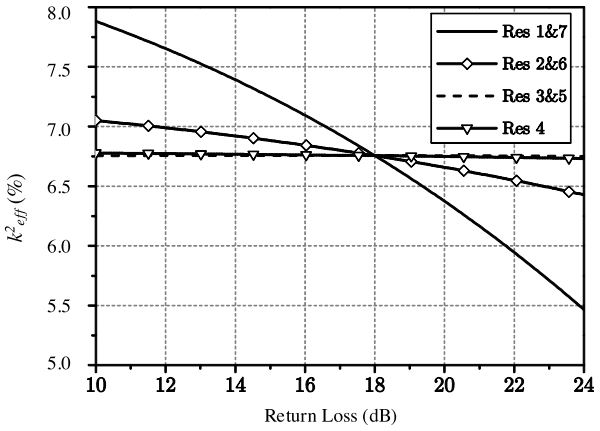

FIGURE 10. Electromechanical coupling coefficient values for a specified vector of finite transmission zeros as a function of *RL* for each resonator of the Rx filter. It can be seen that at *RL*=18 dB the electromechanical coupling constants are equal for all resonators.

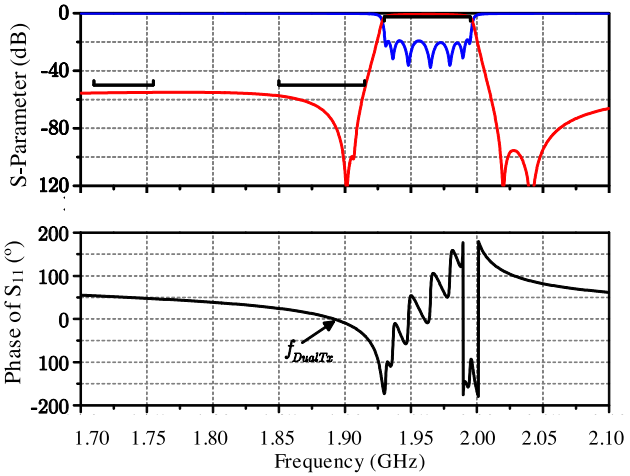

FIGURE 11. S-parameters and $\angle S_{11}$ of the B25 Rx filter. Note that the phase is $\angle S_{11} = 0°$ at f_{DualTx} as it is imposed during the synthesis process. The used quality factor is $Q = 1500$.

$J_{r3} = 1.6264$, $J_{r4} = 2.6951$, and $b_i = \Omega_i$, the normalized transmission zeros. All the couplings between NRNs are set to 1, and the input/output external elements are B_{in}, $B_{out} = -1.0004$.

Once the lowpass elements are obtained, the next step is to carry out the frequency transformation to obtain the elements for the BVD equivalent circuit. Such transformed elements are found in Table 2. Fig. 11 shows the results for the simulation of the S-parameters and the phase for the synthesized bandpass Rx filter. As it is expected, the phase is $\angle S_{11} = 0°$ at the center frequency of the Tx band f_{DualTx}.

TABLE 2. Synthesized BVD bandpass elements of the B25Rx Filter.

BVD Element	Res 1&7	Res 2&6	Res 3&5	Res 4
L_A (nH)	99.71	16.74	104.20	17.08
C_A (pF)	64.56	418.62	63.09	407.95
C_0 (pF)	1.09	7.12	1.07	6.94
$L_{in/out}$	4.053			
k^2_{eff} (%)	6.76	6.76	6.76	6.76
f_s (GHz)	1.984	1.901	1.963	1.906

When the Rx is designed, an adequate transmission zeros and return loss for the Tx has to be found to satisfy the technological requirements and the masks specifications as it was done previously. Contrary to Rx filter, the solution found for the transmitter results in the need of one additional lumped element to resonator 4, due to its electromechanical coupling constant differs of the technological required one, as it is shown in Table 3. Such element is found to be $L_{ext} = 0.789$nH. Fig. 12 shows the S-parameters of the bandpass Tx filter and the phase of the reflection coefficient. Note that the masks specifications are satisfied, and the phase is $\angle S_{11} = 0°$ at the center frequency of the Rx f_{DualRx}.

In Fig. 13 there are represented the duplexer network resulting from the synthesis, where the input/output inductor

TABLE 3. Synthesized BVD bandpass elements of the B25Tx Filter.

BVD Element	Res 1&7	Res 2&6	Res 3&5	Res 4
L_A (nH)	72.06	35.98	200.66	11.16
C_A (pF)	99.06	211.96	35.47	704.39
C_0 (pF)	1.68	3.60	0.60	6.62
$L_{in/out}$	18.15			
k^2_{eff} (%)	6.76	6.75	6.76	11.57
f_s (GHz)	1.884	1.823	1.886	1.795

inductors, and the inductor coil to ground on forth resonator of the transmitter can be appreciated. Notice that, at antenna port the Rx and Tx input coil inductors can be merged in only one reactive element, and at the output port of the Tx filter the shunt inductor could be neglected due to its high value. The duplexer's transmission response is shown in Fig. 14(a). Note that it satisfies the masks specifications, whereas the electromechanical coupling constant of all resonators are $k^2_{eff} = 6.76\%$ with the need of only one external element. Fig. 14(b) shows the isolation between the Tx and Rx bands below 65 dB, better than the 60 dB required for this application.

VI. DESIGN AND VALIDATION OF A STAND-ALONE FILTER FOR THE B28RX BAND

With the aim to carry out the experimental validation of the proposed methodology for the synthesis of AW filters, a B28Rx stand-alone filter has been designed and compared with the fabricated prototype. As it was previously discussed, the objective is to deal with the accommodation of the technological constraints, so, the nature and allocation of required external reactive elements is also provided by the methodology.

The order of the filter is $N = 7$, and the predefined vector of finite transmission zeros to accommodate the technological constraints, but also to achieve mask fulfillment are: $\Omega_1 = -1.113$, $\Omega_2 = 1.754$, $\Omega_3 = -1.102$, $\Omega_4 =$

TABLE 4. Obtained resonator characteristics from the proposed synthesis methodology.

f_s [GHz]	k^2_{eff} [%]	C_0 [pF]	f_s [GHz]	k^2_{eff} [%]	C_0 [pF]	C_{ext} [pF]	L_{ext} [nH]
0.749	13.81	0.757	0.749	13.81	0.757	0	0
0.780	14.77	2.202	0.780	14.77	2.202	0	0
0.750	6.37	3.697	0.750	14.30	1.508	2.189	0
0.786	8.86	2.836	0.786	13.70	1.736	1.100	0
0.735	14.75	6.807	0.735	14.75	6.807	0	0
0.785	13.86	1.195	0.785	13.86	1.195	0	0
0.720	24.53	3.930	0.720	14.67	2.217	0	8.161

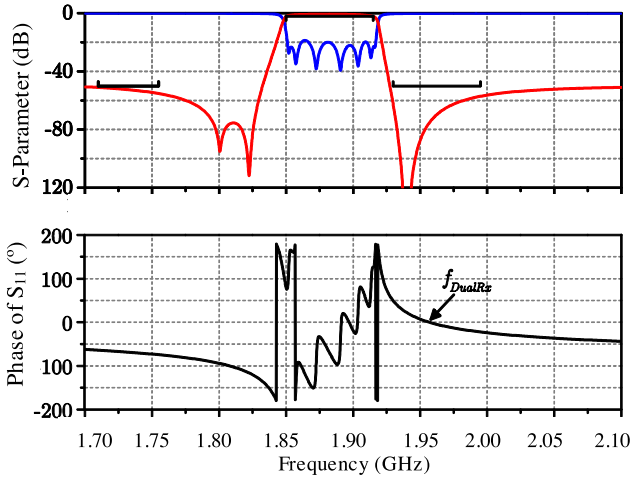

FIGURE 12. S-parameters and $\angle S_{11}$ of the B25 Tx filter. Note that the phase is $\angle S_{11} = 0°$ degrees at f_{DualRx} as it is imposed during the synthesis process. The used quality factor is $Q = 1500$.

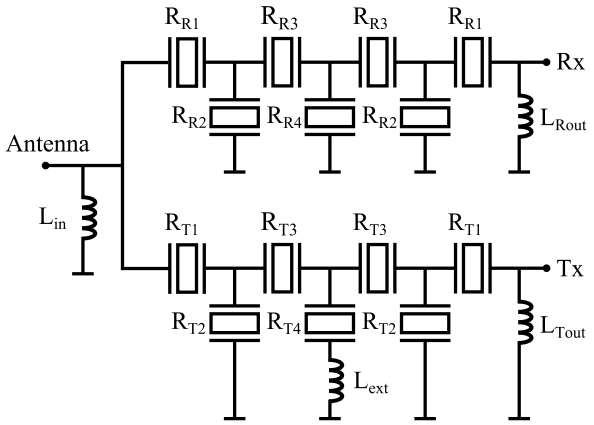

FIGURE 13. Network of the synthesized B25 duplexer, with the input and output inductor coil (the output inductor coil in the Tx path can be neglected).

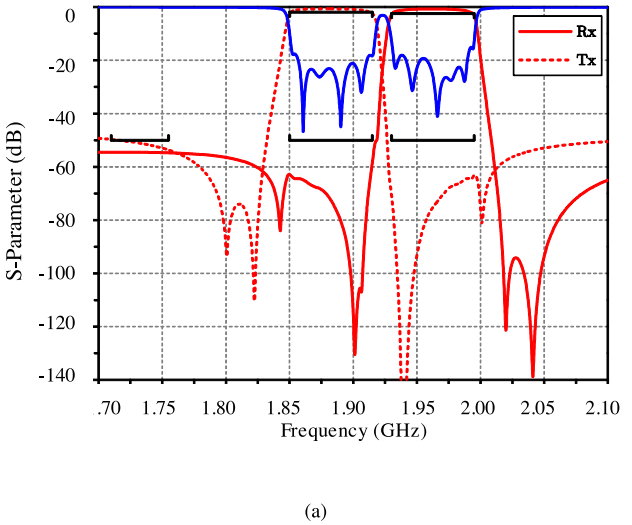

FIGURE 14. Simulation of the duplexer, considering a Q=1500 for the resonators and Q=25 for the inductor coils. (a) Transmission response, and (b) isolation between bands.

1.193, $\Omega_5 = -1.650$, $\Omega_6 = 1.836$ and $\Omega_7 = -2.20$. In this case, the first transmission zero is negative which corresponds to a shunt resonator. Table 4 show the obtained values once the proposed synthesis methodology is applied. In this case, the objective electromechanical coupling constant is $k^2_{eff} = 14.3\%$.

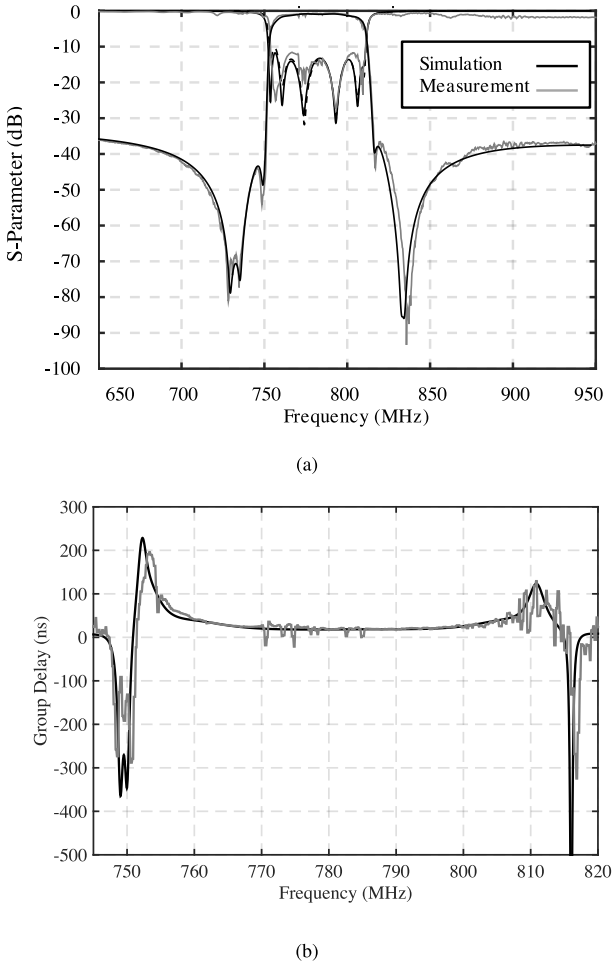

FIGURE 15. Comparison between the simulated network from the synthesis methodology (black line) and measured fabricated filter (gray line) for the B28Rx Band. (a) Transmission response, and (b) in-band group delay.

On the left part of Table 4, the resonance frequency f_s, the electromechanical coupling constant k^2_{eff} and the static capacitance C_0 are found. As seen, to fulfill mask specifications, the required k^2_{eff} for resonators 3 and 4 is higher than the reference value, while it is lower for resonator 7. The required external reactive elements to accommodate the technological constraints are found in the right part of the Table 4. In this case, the high value for shunt inductor with resonator 7 allows to neglect it without degradation of the filter response.

Fig. 15(a) shows the comparison of the simulated network obtained with the synthesis methodology and the fabricated filter at RF360 facilities. In general, there is a very good agreement between both. It must be highlighted that the parasitic effects due to the layout are not considered in the network simulation which lead to some differences between both responses. Also the in-band group delay is found in Fig. 15(b). As it occurs with the transmission response, the agreement between both magnitudes is very good.

VII. CONCLUSION

In this work a general synthesis methodology for the design of AW ladder-type filters is presented. This is based on the extracted pole technique for in-line topologies where NRN are also included. The proposed methodology results in a solution which combines mask specifications fulfillment while accommodating technological constraints of acoustic wave technologies. The methodology has been developed natively oriented to manage the technology constraints, always under the rigorous synthesis foundations.

A lowpass nodal based network made up of resonant and non-resonant nodes is presented. The lowpass electrical model of the acoustic resonator is connected to the bandpass BVD acoustic resonator.

The general methodology has been successfully evaluated to design stand-alone filters without the need of external matching reactive elements at source and load ports, with the proper evaluation of the input phase of the reflection coefficient. But the phase of the reflection coefficient can also be set to achieve high isolation between adjacent bands in the duplexer design. The validation example demonstrates the accuracy of the technique and models, but also the capability of predict the nature and allocation of external reactive elements to accommodate technological constraints.

REFERENCES

[1] S. Mahon, "The 5G effect on RF filter technologies," *IEEE Trans. Semicond. Manuf.*, vol. 30, no. 4, pp. 494–499, Nov. 2017.
[2] F. M. Pitschi, J. E. Kiwitt, R. D. Koch, B. Bader, K. Wagner, and R. Weigel, "High performance microwave acoustic components for mobile radios," in *Proc. IEEE Int. Ultrason. Symp.*, Sep. 2009, pp. 1–10.
[3] U. Bauernschmitt *et al.*, "Advanced microwave acoustic filters enabling advanced system concepts," in *Proc. 58th Electron. Compon. Technol. Conf.*, May 2008, pp. 706–712.
[4] T. Bauer, C. Eggs, K. Wagner, and P. Hagn, "A bright outlook for acoustic filtering: A new generation of very low-profile SAW, TC SAW, and BAW devices for module integration," *IEEE Microw. Mag.*, vol. 16, no. 7, pp. 73–81, Aug. 2015.
[5] D. R. Pehlke and K. Walsh, "LTE-advanced pro RF front-end implementations to meet emerging carrier aggregation and DL MIMO requirements," *IEEE Commun. Mag.*, vol. 55, no. 4, pp. 134–141, Apr. 2017.
[6] M. Li *et al.*, "A fully matched LTE-A carrier aggregation quadplexer based on BAW and SAW technologies," in *Proc. IEEE Ultrason. Symp.*, Sep. 2014, pp. 77–80.
[7] M. Li, C. Bildl, B. Schleicher, T. Purtova, S. Weigand, and A. Link, "A co-designed Band 1-Band 3 carrier aggregation power amplifier quadplexer in GaAs-HBT and BAW technologies," in *IEEE MTT-S Int. Microw. Symp. Dig.*, May 2016, pp. 1–3.
[8] G. G. Fattinger *et al.*, "Carrier aggregation and its challenges—Or: The golden age for acoustic filters," in *IEEE MTT-S Int. Microw. Symp. Dig.*, May 2016, pp. 1–4.
[9] A. Triano, J. Verdú, P. de Paco, T. Bauer, and K. Wagner, "Relation between electromagnetic coupling effects and network synthesis for AW ladder type filters," in *Proc. IEEE Int. Ultrason. Symp. (IUS)*, Sep. 2017, pp. 1–4, doi: 10.1109/ULTSYM.2017.8091644.
[10] M. J. Blasco, "A coupling matrix vision for mobile filtering devices with micro-acoustic wave technologies. A systematic approach," Ph.D. dissertation, Dept. Telecomun. Eng. Sistemes, Univ. Autòn. Barcelona, Bellaterra, Spain, 2015.
[11] A. R. G. Bonastre, "RF filters and multiplexers based on acoustic wave technologies with ladder-type and cross-coupled topologies," Ph.D. dissertation, Dept. Telecomun. Eng. Sistemes, Univ. Autòn. Barcelona, Bellaterra, Spain, 2016.

[12] C. M. Kudsia, R. J. Cameron, and R. Mansour, *Microwave Filters for Communication Systems: Fundamentals, Design and Applications*. Hoboken, NJ, USA: Wiley, 2007.
[13] R. J. Cameron, "Advanced filter synthesis," *IEEE Microw. Mag.*, vol. 12, no. 6, pp. 42–61, Oct. 2011.
[14] R. J. Cameron, A. R. Harish, and C. J. Radcliffe, "Synthesis of advanced microwave filters without diagonal cross-couplings," *IEEE Trans. Microw. Theory Techn.*, vol. 50, no. 12, pp. 2862–2872, Dec. 2002.
[15] R. J. Cameron, "Advanced coupling matrix synthesis techniques for microwave filters," *IEEE Trans. Microw. Theory Techn.*, vol. 51, no. 1, pp. 1–10, Jul. 2003.
[16] V. Miraftab and M. Yu, "Advanced coupling matrix and admittance function synthesis techniques for dissipative microwave filters," *IEEE Trans. Microw. Theory Techn.*, vol. 57, no. 10, pp. 2429–2438, Oct. 2009.
[17] S. Amari and G. Macchiarella, "Synthesis of inline filters with arbitrarily placed attenuation poles by using nonresonating nodes," *IEEE Trans. Microw. Theory Techn.*, vol. 53, no. 10, pp. 3075–3081, Oct. 2005.
[18] S. Tamiazzo and G. Macchiarella, "Synthesis of cross-coupled prototype filters including resonant and non-resonant nodes," *IEEE Trans. Microw. Theory Techn.*, vol. 63, no. 10, pp. 3408–3415, Oct. 2015.
[19] Y. Yang, M. Yu, and Q. Wu, "Advanced synthesis technique for extracted pole and NRN filters," in *IEEE MTT-S Int. Microw. Symp. Dig.*, May 2016, pp. 1–4.
[20] Y. Yang, M. Yu, and Q. Wu, "Advanced synthesis technique for unified extracted pole filters," *IEEE Trans. Microw. Theory Techn.*, vol. 64, no. 12, pp. 4463–4472, Dec. 2016.
[21] K.-Y. Hashimoto, *RF Bulk Acoustic Wave Filters for Communications*. Norwood, MA, USA: Artech House, 2009.
[22] R. Ruby, "11E-2 review and comparison of bulk acoustic wave FBAR, SMR technology," in *Proc. IEEE Ultrason. Symp.*, Oct. 2007, pp. 1029–1040.
[23] P. Warder and A. Link, "Golden age for filter design: Innovative and proven approaches for acoustic filter, duplexer, and multiplexer design," *IEEE Microw. Mag.*, vol. 16, no. 7, pp. 60–72, Aug. 2015.
[24] C. C. W. Ruppel, "Acoustic wave filter technology–A review," *IEEE Trans. Ultrason., Ferroelectr., Freq. Control*, vol. 64, no. 9, pp. 1390–1400, Sep. 2017.
[25] O. Menéndez, P. de Paco, R. Villarino, and J. Parron, "Closed-form expressions for the design of ladder-type FBAR filters," *IEEE Microw. Wireless Compon. Lett.*, vol. 16, no. 1, pp. 657–659, Dec. 2006.
[26] O. Menéndez, P. de Paco, E. Corrales, and J. Verdú, "Procedure for the design of ladder BAW filters taking electrodes into account," *Prog. Electromagn. Res. Lett.*, vol. 7, pp. 127–137, 2009.
[27] O. Menéndez, P. de Paco, J. Gemio, J. Verdú, and E. Corrales, "Methodology for designing microwave acoustic filters with Butterworth/Chebyshev response," *Int. J. Microw. Wireless Technol.*, vol. 1, no. 1, pp. 11–18, 2009.
[28] J. Verdú, P. de Paco, and O. Menéndez, "Electric equivalent circuit for the thickened edge load solution in a bulk acoustic wave resonator," *Prog. Electromagn. Res.*, vol. 11, pp. 13–23, 2010.
[29] J. Verdú, O. Menéndez, and P. de Paco, "Ladder-type filter based on bulk acoustic wave resonators with improved out-of-band rejection," *Microw. Opt. Technol. Lett.*, vol. 50, no. 1, pp. 103–107, Jan. 2008.
[30] J. Verdú, I. Evdokimova, P. de Paco, T. Bauer, and K. Wagner, "Synthesis methodology for the design of acoustic wave stand-alone ladder filters, duplexers and multiplexers," in *Proc. IEEE Int. Ultrason. Symp. (IUS)*, Sep. 2017, pp. 1–4, doi: 10.1109/ULTSYM.2017.8092144.
[31] W. Mueller and R. Ruby, "Multiplexers as a method of supporting same-frequency-range down link carrier aggregation," in *IEEE MTT-S Int. Microw. Symp. Dig.*, May 2016, pp. 1–4.
[32] N. Shibagaki, K. Sakiyama, and M. Hikita, "SAW antenna duplexer module using SAW-resonator-coupled filter for PCN system," in *Proc. IEEE Ultrason. Symp.*, vol. 1, Oct. 1998, pp. 13–16.
[33] G. Fattinger, A. Volatier, R. Aigner, and F. Dumont, "BAW PCS-duplexer chipset and duplexer applications," in *Proc. IEEE Ultrason. Symp.*, Nov. 2008, pp. 602–606.
[34] J. D. Larson, P. D. Bradley, S. Wartenberg, and R. C. Ruby, "Modified butterworth-van dyke circuit for FBAR resonators and automated measurement system," in *Proc. IEEE Ultrason. Symp.*, Oct. 2000, pp. 863–868, doi: 10.1109/ULTSYM.2000.922679.
[35] J.-S. Hong and M. Lancaster, *Microstrip Filters for RF/Microwave Applications*. Hoboken, NJ, USA: Wiley, 2001.
[36] I. Evdokimova, A. Gimenez, J. Verdú, and P. de Paco, "Synthesis of ladder-type acoustic filters in the band-pass domain," in *Proc. 47th Eur. Microw. Conf. (EuMC)*, Oct. 2017, pp. 640–643.
[37] R. J. Cameron, "General coupling matrix synthesis methods for Chebyshev filtering functions," *IEEE Trans. Microw. Theory Techn.*, vol. 47, no. 4, pp. 433–442, Apr. 1999.
[38] D. M. Pozar, *Microwave Engineering*. Hoboken, NJ, USA: Wiley, 2005.
[39] A. Volatier, G. Fattinger, F. Dumont, P. Stoyanov, and R. Aigner, "Technology enhancements for high performance BAW duplexer," in *Proc. IEEE Int. Ultrason. Symp. (IUS)*, Jul. 2013, pp. 761–764.

ALFRED GIMÉNEZ was born in Lleida, Spain, in 1988. He received the M.S. degree in electrical engineering, the M.S. degree in micro and nano electronic engineering, and the Ph.D. degree *(cum laude)* from the Universitat Autònoma de Barcelona (UAB), Barcelona, Spain, in 2012, 2013, and 2016, respectively. In 2012, he joined the Antenna and Microwave Systems Group, Telecommunications and Systems Engineering Department, UAB. His main research interests include computer-aided design of microwave filters, novel synthesis techniques, and BAW and SAW devices.

JORDI VERDÚ (M'18) was born in Sabadell, Spain, in 1980. He received the M.S. degree in telecommunication engineering and the Ph.D. degree *(cum laude)* from the Universitat Politècnica de Catalunya (UPC), in 2006 and 2010, respectively. From 2006 to 2010, he was a member of the Antenna and Microwave Systems. In 2010, he joined the RF System Group, European Spallation Source in Bilbao, where he was a Group Coordinator. From 2011 to 2012, he was with the École Polytechnique fédérale de Lausanne through a Marie Curie Grant. In 2013, he joined the Theory Signal Communication Group, UPC. Since 2015, he became a Visitant Professor at the Universitat Autònoma de Barcelona , where he teaches microwave engineering courses. He was a recipient of the Department Best Thesis Prize for his Ph.D. degree.

His current research interests include the design of planar microwave devices and acoustic wave filters-based in BAW and SAW technologies, from the resonator design point of view, but also from the filter synthesis using novel design techniques.

PEDRO DE PACO SÁNCHEZ was born in Badalona, Spain. He received the M.S. degree in telecommunication engineering and the Ph.D. degree *(cum laude)* from the Universitat Politècnica de Catalunya (UPC), in 1997 and 2003, respectively.

In 1998, he joined the Electromagnetic and Photonics Engineering Group (EEF), Signal Theory and Communications Department, UPC, with a grant from the Institut d'Estudis Espacials de Catalunya in a joint activity related with the European Scientific Space Mission Planck. He was a member of the LFI-Radiometer Working Group and the Planck Consortium. Since 1999, he has been a member of the EEF Group, and from 2003 to 2004 he was an Associate Professor at the UPC. Since 2004, he has been a Lecturing Professor at the Universitat Autònoma de Barcelona , where he teaches microwave engineering courses.

He has participated in several national and international research projects mostly related to microwave and millimeter-wave circuits and systems applied to design and testing of remote sensing instruments and front-end point-to-multipoint broad-band

communication systems. His current areas of interests include hybrid and monolithic technologies, device modelling and emerging technologies (metamaterials and MEMS-FBAR) for device miniaturization. He is a member of the Spanish Networks of Antenna (REsA) and a reviewer of several IEEE journals.